The detailed kinetics of the desorption of hydrogen from polycrystalline copper catalysts

J. Tabatabaei [a], B.H. Sakakini [a], M.J. Watson [b] and K.C. Waugh [a]

[a] *Department of Chemistry, Faraday Building, UMIST, PO Box 88, Manchester M60 1QD, UK*
[b] *ICI Katalco RT & E, PO Box 1, Billingham, Cleveland, UK*

Received 18 December 1998; accepted 17 March 1999

The kinetics of desorption of hydrogen from the copper component of an alumina-supported polycrystalline copper catalyst has been studied in detail by temperature-programmed desorption (TPD). Line-shape analysis of the hydrogen TPD spectra shows: (i) that the desorption is second order, (ii) that the desorption activation energy is in the range 64–68 kJ mol^{-1} in the coverage range 7–44% of a monolayer, and (iii) that the desorption pre-exponential term has a value $\sim 10^{-5}$ cm^2 s^{-1} atom^{-1} consistent with the desorption being second order, involving mobile adsorbates and a mobile desorption transition state.

Keywords: hydrogen, desorption, copper, activation energy, kinetics, order of desorption

1. Introduction

Copper has been shown to be the active component in the $Cu/ZnO/Al_2O_3$ methanol synthesis catalyst [1,2]. Radiolabelling studies have shown that it is the CO_2 component of the $CO/CO_2/H_2$ feed which is hydrogenated to methanol [3,4]. This transformation occurs by the hydrogenation of an adsorbed carbonate species to form an adsorbed formate whose subsequent hydrogenation to a methoxy species is the rate-limiting step in the synthesis [5,6]. High-pressure (30 bar) DRIFTS studies in which the $H_2 : CO_2$ ratio was varied from 2 : 1 to 1 : 12 clearly, and surprisingly, demonstrated that at low $H_2 : CO_2$ ratios, even at 30 bar, the reaction is limited by surface population of adsorbed hydrogen [7]. An understanding of the kinetics of hydrogen adsorption and desorption on copper is clearly key to any detailed description of the mechanism of methanol synthesis.

There have been many single-crystal studies on the dynamics of hydrogen adsorption on copper [8–18] with complementary theoretical studies to provide additional detail to this understanding [19–23]. These have determined the activation energies to adsorption and the desorption activation energies on the Cu(111), (110) and (100) surfaces [11–16].

It is clear that the surface of the supported polycrystalline copper which constitutes the active component of the industrial methanol synthesis catalyst will contain a proportion of the low-index surfaces studied in the single-crystal experiments. Whereas the dynamics of adsorption and desorption of hydrogen on these surfaces determined in single experiments will apply when they exist on a polycrystalline surface, the overall kinetics of hydrogen adsorption and desorption on the polycrystalline copper component of the catalyst will be complex and will depend on the relative surface populations of the low-index faces and the populations of higher-index faces for which the single-crystal dynamics of hydrogen adsorption has not yet been obtained. It has been suggested that line-shape analysis of the hydrogen temperature-programmed desorption peak could yield these relative populations [24]. This will only be the case if higher-index faces either do not exist on the surface of the copper or are present to a negligible extent.

The purpose of this study is to determine the detailed kinetics of desorption of hydrogen on polycrystalline copper. The material used in this study is alumina-supported copper rather than the $Cu/ZnO/Al_2O_3$ catalyst to avoid complications of adsorption on ZnO. The order of desorption and the desorption activation energy will be determined by line-shape analysis of the temperature-programmed desorption peaks. The values obtained will be compared with the single-crystal data in an attempt to gain insights into the surface morphology of the polycrystalline copper.

2. Experimental

2.1. The microreactor

The multipurpose microreactor has been described in detail elsewhere [25]. It is a single-tube reactor (20 cm long, 0.4 cm i.d.) connected via a heated capillary to a mass spectrometer (Hiden Analytical, Warrington, England) capable of following 16 masses continuously with temperature/time. In these experiments, the mass to charge ratios $m/z = 2$, 18, 28 and 44 were followed.

The microreactor system is capable of a number of *in situ* measurements. Those used here are: (i) total surface area measurements by N_2 frontal chromatography (FC) at 77 K, (ii) copper metal area measurements by N_2O reactive frontal chromatography (RFC), and (iii) orders of desorption, surface coverages and desorption activation energies

by analysis of temperature-programmed desorption (TPD) line shapes [26].

2.2. The catalysts

Three catalysts were studied. They were: (i) polycrystalline copper, (ii) alumina-supported polycrystalline copper, and (iii) an industrial $Cu/ZnO/Al_2O_3$ methanol synthesis catalyst. All of the catalysts were prepared by ICI.

The polycrystalline copper was prepared in the following way. Copper carbonate was first prepared by precipitation by sodium carbonate addition to copper nitrate solution. The carbonate was filtered and washed free of sodium. It was then dried and calcined in air at 573 K for 3 h. The Cu/Al_2O_3 and the $Cu/ZnO/Al_2O_3$ catalysts were prepared by sodium carbonate precipitation of nitrate solutions of the mixed metals. The filtration, drying, calcination and reduction processes were all identical to that described above for the preparation of polycrystalline copper. Before use, the catalysts were reduced in an H_2/He stream (5% H_2, 25 $cm^3\,min^{-1}$, 1 bar), raising the temperature from ambient to 513 K at 1 $K\,min^{-1}$ and holding the temperature at 513 K for 16 h under the H_2/He stream. The catalysts were then cooled to 77 K under the H_2–He stream. The adsorbed surface hydrogen was removed by temperature-programmed desorption in He.

The total surface area of the Cu/Al_2O_3 (50 : 50) catalyst measured *in situ* by FC was 58 $m^2\,g^{-1}$ and the copper metal area measured by N_2O RFC was 11 m^2/g-cat.

The total surface area of the $Cu/ZnO/Al_2O_3$ (60 : 30 : 10) catalyst was 65 m^2/g-cat. and the copper metal area was 30 m^2/g-cat.

2.3. The gases

Helium was supplied by Linde and was 99.999% pure. Before use, it was passed through a Chromapack Gas Clean moisture filter. Hydrogen–helium (5% H_2 in He) was from ECM and was 99.999% pure.

3. Results and discussion

3.1. Hydrogen desorption from polycrystalline copper (Cu(pc)), alumina-supported copper (Cu/Al_2O_3) and zinc oxide/alumina-supported copper ($Cu/ZnO/Al_2O_3$)

The temperature-programmed desorption spectra of H_2 from Cu(pc) (figure 1(a)), Cu/Al_2O_3 (figure 1(b)) and $Cu/ZnO/Al_2O_3$ (figure 1(c)) were all produced in an identical manner. Having prepared the reduced catalysts as described in section 2, the temperature of each catalyst was lowered to 77 K under the H_2 stream for approximately 30 min. The flow was then switched to a He stream and the temperature of each catalyst was raised from 77 to 600 K at 5 $K\,min^{-1}$.

Two peaks are observed in the H_2 desorption spectrum from Cu(pc) at 280 K (the dominant one) and at 530 K (figure 1(a)). For Cu/Al_2O_3 also two H_2 desorption peaks are

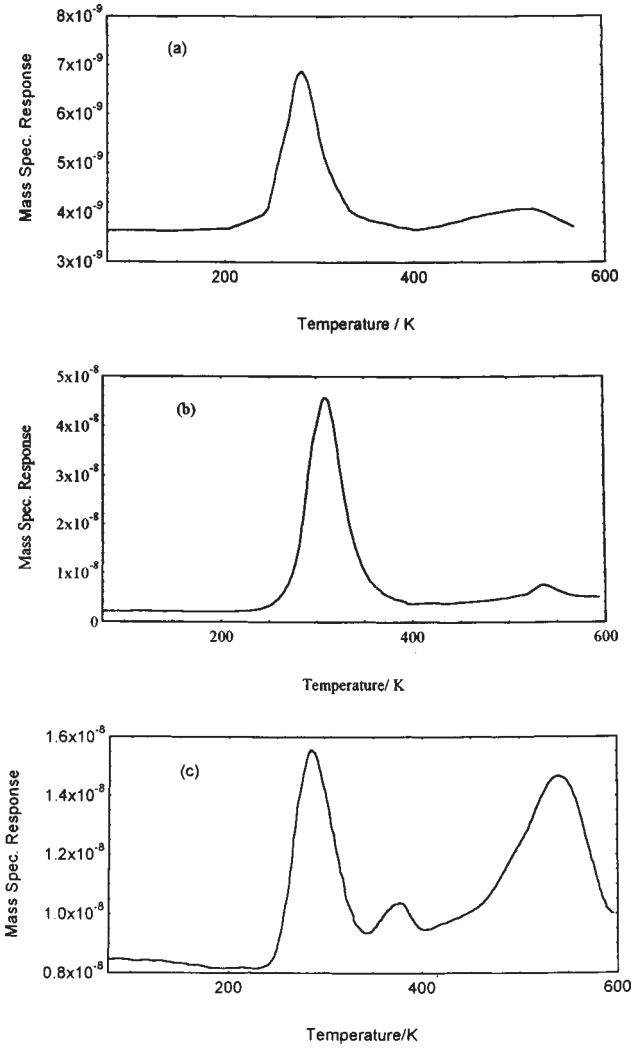

Figure 1. Hydrogen desorption spectra from the reduced CuO (a), CuO/Al_2O_3 (b) and $CuO/ZnO/Al_2O_3$ (c).

observed – at 310 (the dominant one) and at 530 K. Three H_2 desorption peaks are observed from the $Cu/ZnO/Al_2O_3$ catalyst – at 280, 390 and 530 K.

Two peaks are common to all the spectra and so, quite unambiguously can be ascribed to the copper. The peak at ∼300 K derives from hydrogen desorbing from the surface of the copper, the variation in the value of the maxima deriving from different coverages (see below). The approximate value of the maxima, however, indicates that hydrogen is desorbing from a surface which is predominantly Cu(111) (the high-coverage desorption peak maximum of H_2 from Cu(111) is 305 K [11]).

The high-temperature $T_m = 530$ K hydrogen desorption peak obtained from the Cu(pc) and the Cu/Al_2O_3 catalysts probably derives from hydrogen evolving from subsurface layers of the copper metal having been adsorbed during the prolonged reduction at 513 K. Hydrogen corresponding to many adsorbed layers has been observed during CO reduction at 473 K of a hydrated Cu/Al_2O_3 catalyst which had been surface oxidised by N_2O [26]. Additionally, Chorkendorff and co-workers [16] observed H_2 desorption

at 590 K from the bulk of a Cu(100) crystal, the higher peak maximum deriving from a combination of higher heating rate and different morphology.

The $Cu/ZnO/Al_2O_3$ catalyst exhibits a much larger H_2 desorption peak at ∼545 K. This is thought to be due to H_2 desorbing from the bulk of the Cu and also from the bulk of ZnO [27]. In addition, the $Cu/ZnO/Al_2O_3$ catalyst exhibits a H_2 desorption peak at 380 K.

Roberts and Griffin [28,29] and Muhler and co-workers [24] have also observed this peak and have attributed it to hydrogen desorption from copper oxide species resulting from incomplete reduction of the copper oxide. The absence of this peak from the hydrogen desorption spectrum of the Cu/Al_2O_3 catalyst leads us to favour the argument that it derives from some form of interfacial Cu/ZnO type sites [30].

Having shown that the hydrogen desorption peak at ∼300 K derives from desorption from polycrystalline copper, we shall analyse this peak to determine the order and activation energy of hydrogen desorption from alumina-supported polycrystalline copper to avoid the complications engendered by the ZnO.

3.2. Order of desorption of hydrogen from the copper component of the alumina-supported copper (Cu/Al_2O_3)

The Cu/Al_2O_3 catalyst was first reduced in the H_2/He stream, as described in section 2. After completion of the reduction, the temperature was lowered to 77 K under the H_2/He stream. The flow was then switched to He (25 $cm^3\,min^{-1}$) and the temperature was then raised from 77 to 600 K at 5 $K\,min^{-1}$. This desorbed all of the adsorbed hydrogen which had been adventitiously dosed onto the copper surface during cooling from 513 to 77 K in the H_2/He stream. No water nor carbon dioxide was evolved during this temperature programming so that prior to dosing hydrogen in the manner described below, the surface of the catalyst is completely free of hydroxyl species or hydrogen.

The different coverages of the Cu by hydrogen shown in figure 2 were produced by exposing the catalyst to the H_2/He stream (5% H_2 in He, 1 bar, 25 $cm^3\,min^{-1}$) at 273 K for different lengths of time after which the catalyst was cooled from 273 to 173 K in the H_2/He stream, a process which took about 30 min, at the end of which the flow was switched to He and the temperature was raised from 173 to 600 K at 5 $K\,min^{-1}$. Curve (a) of figure 2 was obtained after flowing the H_2/He stream for 3 min at 273 K, curve (b) resulted from 6 min flow at 273 K, and curve (c) from a 10 min flow at 273 K. Line-shape analysis of these desorption peak shapes by the method described below provided the temperature-dependence rates of desorption at given coverages.

The rate of desorption at any temperature is proportional to the height of the peak at that temperature, while the area of the peak after that temperature is proportional to the hydrogen coverage of the copper at that measured rate of

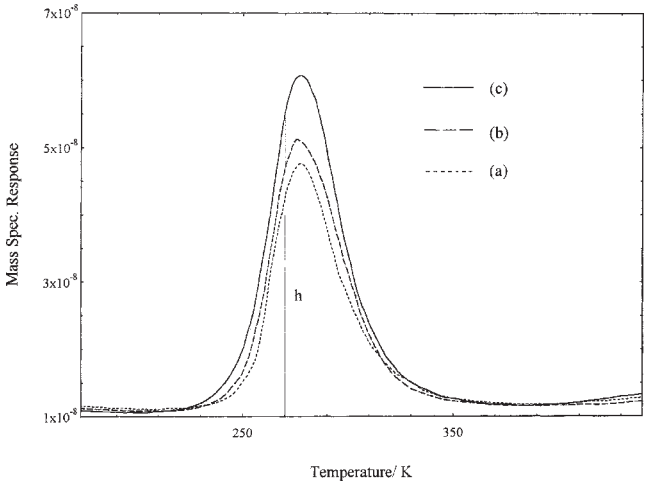

Figure 2. Hydrogen desorption peaks from the Cu component of Cu/Al_2O_3 after dosing hydrogen onto the Cu at 273 K from a H_2/He stream (5% H_2 in He, 25 $cm^3\,min^{-1}$, 1 bar) for 3 min (curve (a)), 6 min (curve (b)) and 10 min (curve (c)).

desorption, e.g., height, h, at 270 K in figure 2. Application of the calibration constants simply transforms the heights of the peaks to rates of desorption and the areas to surface coverages. Table 1 lists the temperatures (K) at which the heights h (cm) were measured, together with their corresponding rates of desorption. It also lists the areas of the peaks (area (cm^2)) after these temperatures and the coverages of the copper by hydrogen corresponding to these areas.

The hydrogen atom coverages of the copper, reported in table 1, which were produced by the different dosing times at 273 K are calculated assuming an average copper atom density of 1.4×10^{19} atom m^{-2} [25].

The order of desorption is given by

$$\frac{dH_{(a)}}{dt} = 2\frac{dH_{2(g)}}{dt} = Ae^{-E_d/RT}H_{(a)}^{n}, \qquad (1)$$

where $dH_{(a)}/dt$ is the rate of desorption (atom $cm^{-2}\,s^{-1}$), A is the desorption pre-exponential whose units depend upon the order of desorption, E_d is the desorption activation energy ($J\,mol^{-1}$), R is the gas constant ($J\,mol^{-1}\,K^{-1}$), $H_{(a)}$ is the hydrogen atom coverage (at cm^{-2}), and n is the order of desorption. Taking logs,

$$\ln\left(-\frac{dH_{(a)}}{dt}\right) = \ln\left(2\,\frac{dH_{2(g)}}{dt}\right) = \ln A - E_d/RT + n\ln H_{(a)}. \qquad (2)$$

A plot of $\ln(2\,dH_{2(g)}/dt)$ versus $\ln H_{(a)}$ at fixed temperatures will have a gradient of n – the order of desorption.

Such a plot is shown in figure 3 for the constant temperatures 260 K (line (a)), 265 K (line (b)), 270 K (line (c)) and 275 K (line (d)). The order of desorption so obtained is 1.8 at 260 K, 2.0 at 265 K, 1.8 at 270 K and 1.9 at 275 K. It is concluded therefore that hydrogen atom desorption from copper is second order.

This experimental confirmation that the desorption is second order is important since it verifies that temperature-

Table 1
The rates and desorption as a function of hydrogen atom coverage used to determine the order of desorption analysis of the hydrogen desorption peak shapes shown in figure 2, calculated by the method described in the text. The different initial hydrogen coverages were produced by dosing the catalyst for different times at 273 K.

T (K)	h (cm)	Rate of desorption $\times 10^{11}$ (molecule $cm^{-2}\,s^{-1}$)	Area (cm^{-2})	$H_{(a)}$ coverage $\times 10^{14}$ (atom cm^{-2})	$\ln(2\,dH_2/dt)$	$\ln H_{(a)}$	Gradient (order)
260	$h_1 = 9.3$	2.9	55.0	4.0	27.0	33.61	1.86
	$h_2 = 7.3$	2.3	51.2	3.8	26.9	33.50	
	$h_3 = 3.8$	1.1	33.1	2.4	26.1	33.11	
265	$h_1 = 11.8$	3.8	51.2	3.8	27.4	33.57	1.92
	$h_2 = 9.6$	3.0	48.0	3.6	27.2	33.51	
	$h_3 = 4.7$	1.4	31.8	2.2	26.3	33.02	
270	$h_1 = 14.0$	4.4	48.0	3.6	27.5	33.51	1.87
	$h_2 = 10.8$	3.4	44.2	3.2	27.3	33.30	
	$h_3 = 5.7$	1.6	29.2	2.0	26.5	32.95	
275	$h_1 = 15.6$	4.9	35.1	2.6	27.6	33.20	1.87
	$h_2 = 13.6$	4.3	32.3	2.4	27.5	33.10	
	$h_3 = 6.7$	2.1	21.5	1.6	26.7	32.70	

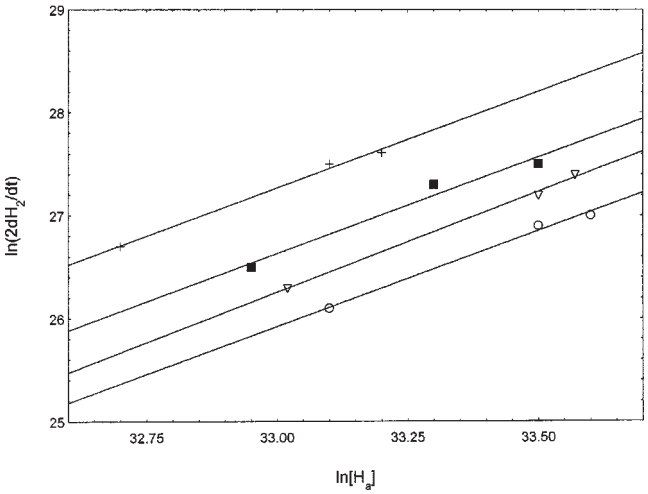

Figure 3. Plots of $\ln(2\,dH_2/dt)$ versus $\ln H_{(a)}$ at constant temperatures of 260 (○), 265 (▽), 270 (■), and 275 K (+).

programmed desorption measurement is a rate measurement and involves no re-adsorption of the hydrogen. Were there to have been significant re-adsorption within the catalyst pores or within the catalyst bed, the measurement would be an equilibrium one. The order of the concentration of hydrogen in the gas phase would be

$$H_{2(g)} = \frac{k_d}{k_a}\frac{\theta^2}{k_a(1-\theta)^2}, \qquad (3)$$

where k_d and k_a are the desorption and adsorption rate constants and θ is the fractional coverage. Equation (3) is second order only in the limit of low θ. Since we are dealing with saturation coverage – which for hydrogen on copper is half monolayer – θ is either 1 or $1/2$. It is not small. Re-adsorption therefore appears not to occur to any significant extent. This can be understood since the measured sticking probabilities of hydrogen on the low-index faces of copper are extremely small ($\sim 10^{-11}$) [13–16]. An important corollary of this near absence of re-adsorption is that the analysis of the line shapes of hydrogen desorption peaks therefore is a valid method for the determination of the desorption activation energy.

3.3. Desorption activation energy of hydrogen from the copper component of the Cu/Al_2O_3 catalyst

A fresh sample of reduced and surface hydrogen desorbed Cu/Al_2O_3 catalyst was dosed with hydrogen from a H_2/He stream (5% H_2 in He, 1 bar, 25 $cm^3\,min^{-1}$, 15 min) at various temperatures in the range 213–333 K, lowering the temperature at the end of the 15 min dosing time from the given adsorption temperature to 173 K under the H_2/He stream for about 30 min. The catalyst was then flushed with He (25 $cm^3\,min^{-1}$, 1 bar) at 173 K for 30 min, after which the temperature was raised from 173 to 500 K at 5 $K\,min^{-1}$ under the He stream, producing the desorption spectra shown in figure 4.

Integration of these spectra shows that the amount of hydrogen adsorbed increases as the adsorption temperature is increased from 213 to 273 K, reflecting the activated nature of the adsorption of hydrogen on copper. Increasing the adsorption temperature above 273 K results in a decrease in the amount of hydrogen adsorbed, showing the measurement now to be thermodynamic rather than kinetic. The maximum value of the $H_{(a)}$/Cu surface ratio obtained at the dosing temperature of 273 K is 0.44, which is slightly smaller than the value of 0.5 obtained for the $H_{(a)}$/Cu surface ratio for Cu(100), (110) and (111) at an adsorption temperature of 190 K [11]. Nevertheless, the value obtained here is slightly higher than that (0.4) predicted by Muhler and co-workers from a consideration of the sticking probabilities of hydrogen on the low-index faces at these temperatures and of the likely surface population of these faces [24].

The desorption peak maximum temperatures shown in figure 4 shift to lower values as the hydrogen coverage increases in agreement with that found by Anger and co-workers [11] and consistent with the desorption being second order [31]. Since the desorption has been shown to be

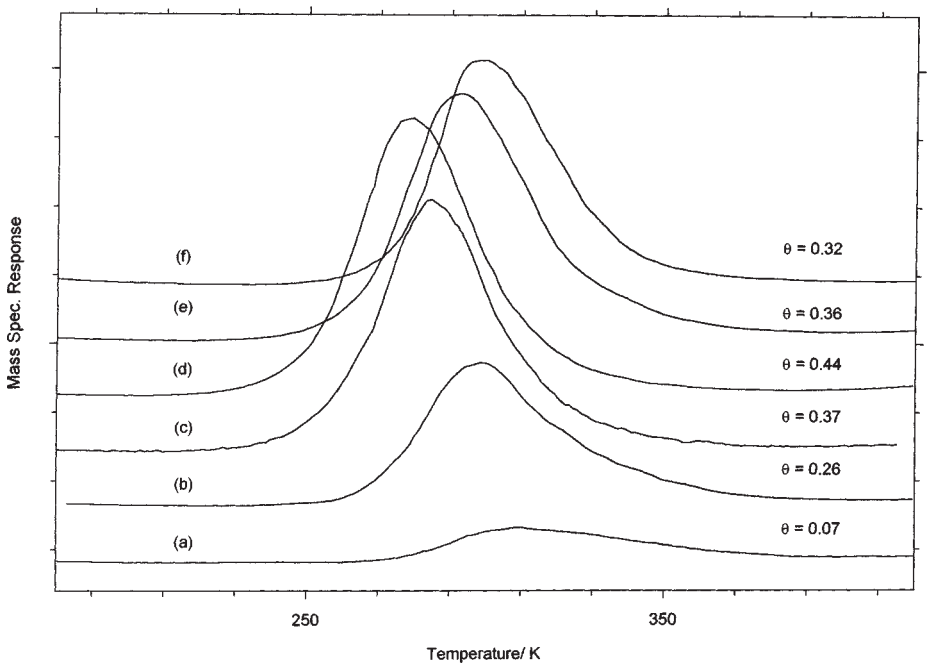

Figure 4. Hydrogen desorption spectra from Cu/Al_2O_3 at dosing temperatures of 213 (a), 233 (b), 253 (c), 273 (d), 303 (e), and 333 K (f).

Table 2
Line-shape analysis of the desorption peaks shown in figure 4 for the determination of the hydrogen desorption activation energy.

Curve	Temperature (K)	h (cm)	Area (cm^2)	$dH_{2(g)}/dt \times 10^{10}$ (molecule $cm^{-2}\,s^{-1}$)	$H_{(a)} \times 10^{14}$ (atom cm^{-2})	$T \times 10^3$ (K)	$\ln(\text{rate}/H^2_{(a)})$	Gradient	E_d ($kJ\,mol^{-1}$)
(a)	$T_1 = 270$	$h_1 = 0.1$	$C_1 = 7.9$	0.50	0.98	3.70	−41.40	8.2	68
	$T_2 = 280$	$h_2 = 0.3$	$C_2 = 7.5$	1.50	0.95	3.57	−40.25		
	$T_3 = 290$	$h_3 = 0.8$	$C_3 = 7.0$	3.75	0.89	3.44	−39.10		
	$T_4 = 300$	$h_4 = 1.2$	$C_4 = 5.0$	6.00	0.78	3.33	−38.60		
(b)	$T_1 = 250$	$h_1 = 0.3$	$C_1 = 29.5$	1.83	3.54	4.00	−42.70	7.9	65
	$T_2 = 260$	$h_2 = 1.0$	$C_2 = 28.5$	5.47	3.47	3.84	−41.60		
	$T_3 = 270$	$h_3 = 2.5$	$C_3 = 25.0$	13.7	3.25	3.70	−40.49		
	$T_4 = 280$	$h_4 = 5.0$	$C_4 = 19.0$	28.0	2.70	3.57	−39.40		
(c)	$T_1 = 250$	$h_1 = 0.5$	$C_1 = 41.0$	2.50	5.06	4.00	−43.00	7.9	65
	$T_2 = 260$	$h_2 = 1.7$	$C_2 = 39.0$	8.71	4.91	3.84	−41.80		
	$T_3 = 270$	$h_3 = 3.8$	$C_3 = 35.0$	19.2	4.49	3.70	−40.70		
	$T_4 = 280$	$h_4 = 7.8$	$C_4 = 25.0$	45.0	3.80	3.57	−39.60		
(d)	$T_1 = 250$	$h_1 = 0.7$	$C_1 = 49.0$	3.10	6.04	4.00	−43.2	7.8	64
	$T_2 = 260$	$h_2 = 1.8$	$C_2 = 47.0$	9.00	5.87	3.84	−42.0		
	$T_3 = 270$	$h_3 = 4.4$	$C_3 = 43.0$	23.9	5.45	3.70	−40.9		
	$T_4 = 280$	$h_4 = 8.8$	$C_4 = 31.0$	48.0	4.50	3.57	−39.9		

second order, the rate of desorption is given by equation (1) in which $n = 2$. The activation energy for desorption can now be obtained by line-shape analysis of the desorption peaks shown in figure 4. This is done by a modification of the method used to obtain the order of desorption. Equation (1) can be rearranged to

$$2\frac{dH_{2(g)}}{dt}\Big/H^2_{(a)} = A e^{-E_d/RT}, \tag{4}$$

$$\ln\left(2\frac{dH_{2(g)}}{dt}\Big/H^2_{(a)}\right) = \ln A - E_d/RT, \tag{5}$$

where E_d ($J\,mol^{-1}$) is the desorption activation energy. Therefore, a plot of $\ln(2(dH_{2(g)}/dt)/H^2_{(a)})$ versus $1/T$ will give the desorption activation energy. As explained previously, the height h (cm) of the peak at any temperature is proportional to $dH_{2(g)}/dt$, while the area (cm^2) of the peak after that temperature is proportional to $H_{(a)}$. Table 2 lists the peak heights and areas together with the derived rates of desorption and hydrogen atom coverages for the temperatures listed.

Plots of $\ln(2(dH_{2(g)}/dt)/H^2_{(a)})$ versus $1/T$ for different initial coverages are shown in figure 5, from which desorption activation energies of 68 $kJ\,mol^{-1}$ (dosing temperature $T_D = 213$ K, $\theta = 0.07$), 65 $kJ\,mol^{-1}$ ($T_D = 233$ K, $\theta = 0.26$), 65 $kJ\,mol^{-1}$ ($T_D = 253$ K, $\theta = 0.37$) and 64 $kJ\,mol^{-1}$ ($T_D = 273$ K, $\theta = 0.44$) are obtained.

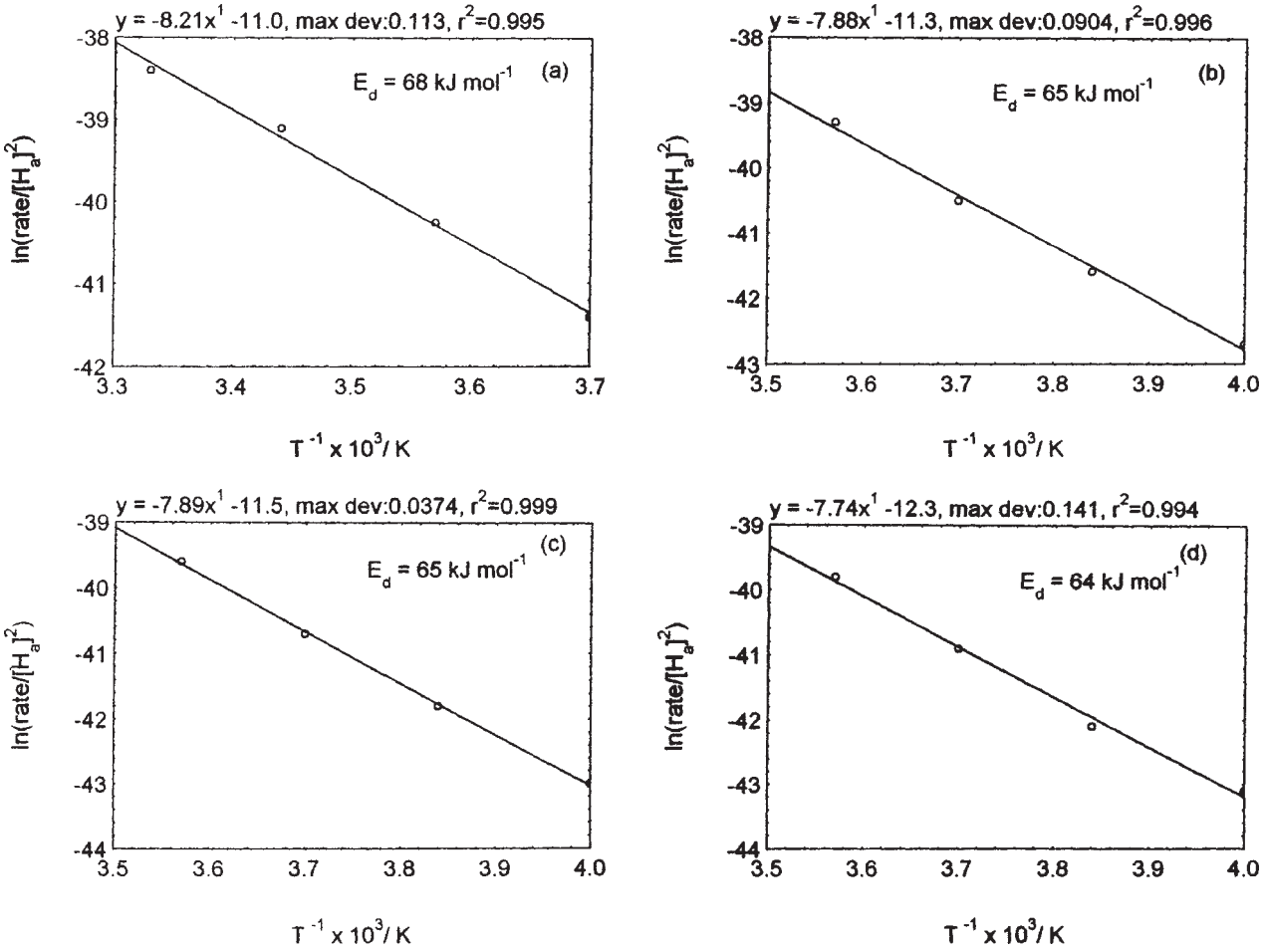

Figure 5. Plots of $\ln(\text{rate}/\text{H}_{(a)}^2)$ versus reciprocal temperature for hydrogen adsorption at 213 (a), 233 (b), 253 (c), and 273 K (d).

Anger and co-workers [11] found values of 72 kJ mol^{-1} falling to 64 kJ mol^{-1} in the coverage range 0.01–0.4 monolayers for Cu(111). The values obtained here lie in this range. A lower estimate of the activation energy to the adsorption of hydrogen on polycrystalline copper can be obtained from the temperature dependence of the hydrogen coverage in the low-temperature dosing regime (213 and 233 K) when only a small fraction of the hydrogen will desorb during the 15 min dosing time at these temperatures. The value obtained is 27 kJ mol^{-1}, which is slightly higher than that of Balooch and co-workers [10] and of Anger and co-workers [11] but lower than the more accurate values of Campbell and Campbell (57 kJ mol^{-1}) and of Hayden and Lamont (60 kJ mol^{-1}) [13–15] and of Chorkendorff and co-workers (48 kJ mol^{-1}) [16]. (Table 2 lists the heights (cm) and the areas (cm^2) used in these calculations together with the corresponding rates of desorption (molecule s^{-1}) and the hydrogen coverages (atom cm^{-2}).)

The intercept of the plots is $\ln A$, where A is the desorption pre-exponential term which for a second-order desorption has units of cm^2 s^{-1} mol^{-1}. The intercept has values of -11 ($\theta = 0.07$), -11.3 ($\theta = 0.26$), -11.5 ($\theta = 0.37$) and -12.3 ($\theta = 0.44$) from which the desorption pre-exponential term has a value of $\sim 10^{-5}$ cm^2 s^{-1} atom^{-1}.

Application of transition state theory for the recombinative desorption of atoms which are mobile leading to a mobile molecular transition state produces equation (3) for the rate of desorption, $\text{dH}_{2(g)}/\text{d}t$:

$$\frac{\text{dH}_{2(g)}}{\text{d}t} = \frac{kT}{h}\frac{q^2_{\text{trans H}^{\#}_{2(a)}}}{q^2_{\text{trans H}_{(a)}} q^2_{\text{trans H}_{(a)}}} \text{e}^{-E^{\#}/kT}\text{H}^2_{(a)}, \qquad (6)$$

where $q_{\text{trans H}}$ is the translational partition of the mobile adsorbed hydrogen atoms, $q_{\text{trans H}^{\#}_{2(a)}}$ is the translational partition function of the mobile $\text{H}^{\#}_{2(a)}$ transition state, k is Boltzmann's constant, $E^{\#}$ is the activation energy to the formation of the mobile transition state and T (K) is the temperature [32].

Since $q^2_{\text{trans H}_{(a)}} = 2q^2_{\text{trans H}^{\#}_{2(a)}}$, the desorption pre-exponential term A_{d} is

$$A_{\text{d}} = \frac{kT}{h}\frac{1}{2q^2_{\text{trans H}_{(a)}}}, \qquad (7)$$

where

$$q^2_{\text{trans H}_{(a)}} = \frac{2\pi mkT}{h^2}; \qquad (8)$$

then A_d has a value of 3.1×10^{-4} $cm^2\,s^{-1}\,atom^{-1}$. This theoretical value is in good agreement with that (10^{-5} $cm^2\,s^{-1}\,atom^{-1}$) found experimentally.

4. Conclusions

1. Analysis of the line shapes of the temperature-programmed desorption peaks of hydrogen from the copper component of a Cu/Al_2O_3 catalyst in which the hydrogen was adsorbed for different dosing times at 273 K has shown the desorption to be second order. This confirmed the qualitative conclusion to this effect, derived from the observation of the movement of the desorption peak maximum temperature to lower temperatures with increasing hydrogen coverage [31]. The value of the desorption pre-exponential obtained in this work (10^{-5} $cm^2\,s^{-1}\,atom^{-1}$) is consistent with a second-order model in which the recombining hydrogen atoms and the molecular hydrogen transition state are mobile on the surface.

2. A corollary of this observation of the second-order nature of the desorption is that negligible re-adsorption of the hydrogen will have occurred on the Cu/Al_2O_3 catalyst either within the pores in the catalyst plug during the desorption. This validates the method of temperature-programmed desorption as a means of obtaining desorption activation energies for this adsorbate from this catalyst.

3. Analysis of the desorption line shapes for significantly different initial hydrogen coverages of the copper produced by dosing on the hydrogen for the same time and different adsorption temperatures shows the desorption activation energy to be only weakly dependent on the initial coverage, having a value of 68 $kJ\,mol^{-1}$ for an initial fractional coverage, θ_i, of 0.07 of a monolayer falling to 64 $kJ\,mol^{-1}$ for $\theta_i = 0.44$. These values are comparable to those of Anger and co-workers [11] for Cu(111). They found a low-coverage ($\sim$0.01 monolayer) desorption activation energy of 72 $kJ\,mol^{-1}$ and a high-coverage one ($\sim$0.4 monolayer) of 64 $kJ\,mol^{-1}$, suggesting that the Al_2O_3-supported polycrystalline copper surface has preponderance of the Cu(111) face.

References

[1] W.X. Pan, R. Cao, D.L. Roberts and G.L. Griffin, J. Catal. 114 (1988) 440.
[2] G.C. Chinchen, K.C. Waugh and D.A. Whan, Appl. Catal. 25 (1986) 101.
[3] Yu.B. Kagan, L.G. Liberov, E.V. Slivinski, S.M. Lockev, G.I. Lin, A.Ya. Rozovsky and A.N. Bashirov, Dokl. Akad. Nauk SSSR 221 (1975) 1093.
[4] G.C. Chinchen, P.J. Denny, D.G. Parker, G.D. Short, M.S. Spencer, K.C. Waugh and D.A. Whan, Prepr. Am. Chem. Soc. Div. Fuel Chem. 29 (1984) 178.
[5] G.J. Millar, C.H. Rochester, C. Howe and K.C. Waugh, J. Mol. Phys. 76 (1991) 833.
[6] M. Bowker, R.A. Hadden, H. Houghton, J.N.K. Hyland and K.C. Waugh, J. Catal. 109 (1988) 263.
[7] S. Bailey, G.F. Froment, J.W. Snoeck and K.C. Waugh, Catal. Lett. 30 (1995) 99.
[8] J. Pritchard, T. Catterick and R.K. Gupta, Surf. Sci. 53 (1975) 1.
[9] I.E. Wachs and R.J. Madix, J. Catal. 53 (1978) 208.
[10] M. Balooch, M.J. Cardillo, D.R. Miller and R.E. Stickney, Surf. Sci. 46 (1974) 358.
[11] G. Anger, A. Winkler and K.D. Rendulic, Surf. Sci. 220 (1989) 1.
[12] J.M. Campbell and C.T. Campbell, Surf. Sci. 259 (1991) 1.
[13] B.E. Hayden and C.L.A. Lamont, Chem. Phys. Lett. 160 (1989) 331.
[14] B.E. Hayden and C.L.A. Lamont, Phys. Rev. Lett. 63 (1989) 1823.
[15] B.E. Hayden, D. Lackey and J. Schott, Surf. Sci. 239 (1990) 119.
[16] P.B. Rasmussen, P.M. Holmblad, H. Christoffersen, P.A. Taylor and I. Chorkendorff, Surf. Sci. 287/288 (1993) 79.
[17] F. Besenbacher, P.T. Sprunger, L. Raun, L. Olesen, I. Stensgaard and E. Loegsgaard, Topics Catal. 1 (1994) 325.
[18] K.H. Rieder and W. Stocker, Phys. Rev. Lett. 57 (1986) 2548.
[19] A.R. Gregory, A. Gelb and R. Silbey, Surf. Sci. 74 (1978) 497.
[20] M.R. Hand and S. Holloway, J. Chem. Phys. 91 (1989) 7209.
[21] G.R. Darling and S. Holloway, J. Chem. Phys. 101 (1994) 3268.
[22] G. Mills and H. Jonsson, Phys. Rev. Lett. 72 (1994) 1124.
[23] G. Wiesenekker, G.J. Kroes, E.J. Baerends and R.C. Mowrey, J. Chem. Phys. 102 (1995) 3873.
[24] M. Muhler, L.P. Nielsen, E. Tornqvist, B.S. Clausen and H. Topsøe, Catal. Lett. 14 (1992) 241.
[25] G.C. Chinchen, C.M. Hay, H.D. Vandervell and K.C. Waugh, J. Catal. 103 (1987) 79.
[26] K.C. Waugh, Appl. Catal. 43 (1988) 315.
[27] G.J. Millar, C.H. Rochester, S. Bailey and K.C. Waugh, J. Chem. Soc. Faraday Trans. 89 (1993) 1109.
[28] D.L. Roberts and G.L. Griffin, Appl. Surf. Sci. 19 (1984) 298.
[29] D.L. Roberts and G.L. Griffin, J. Catal. 110 (1988) 117.
[30] R.A. Hadden, B. Sakakini, J. Tabatabaei and K.C. Waugh, Catal. Lett. 44 (1997) 145.
[31] P.A. Redhead, Trans. Faraday Soc. 57 (1961) 641.
[32] K.C. Waugh, *Elementary Reaction Steps in Heterogeneous Catalysis*, Series C: Math. Phys. Sci. 398 (1993) 407.